Centrifuge study of spill-through abutments

Etude de centrifugation des appuis ouverts

M. F. RANDOLPH, Cambridge University Engineering Department, Cambridge, UK
C. Y. AH-TECK, Sir Alexander Gibb & Partners, Mauritius
R. T. MURRAY, Transport and Road Research Laboratory, Crowthorne, UK

SYNOPSIS One of the most common types of bridge abutment employed in road construction is the open or spill-through abutment. The design approach for this type of abutment was originally developed in 1948, and it is somewhat surprising that the method of design has remained virtually unchanged since that time, in view of the major developments in geotechnical engineering that have occurred. In this paper, the results of a centrifugal model study into the behaviour of spill-through abutments at collapse are presented and a revised approach to their design proposed.

INTRODUCTION

A bridge abutment is an important structural element which serves the dual purpose of supporting the bridge superstructure, and retaining the embankment fill, thus providing a smooth transition from roadway to bridge deck. The lateral thrust from the embankment fill against a traditional retaining wall abutment will generally exceed any possible horizontal loading from the bridge deck, and may prove a critical feature in design of the abutment. As an alternative, the wall may be replaced by a number of piers, with the embankment allowed to 'spill-through' the openings to form a sloping end. This type of abutment, which is one of the most common types currently used, has come to be known as an 'open' or 'spill-through' abutment. Figure 1 shows a typical cross-section.

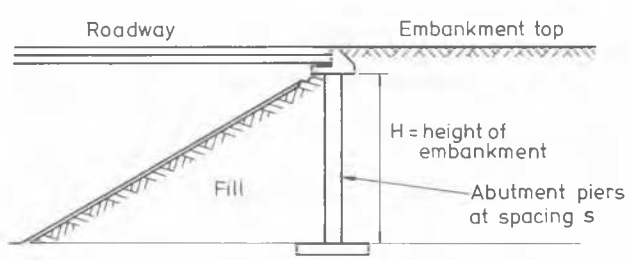

Fig. 1 Typical Spill-through Abutment

The present design approach is based largely on suggestions by Chettoe and Adams (1938), who proposed a design to withstand fully active earth pressures acting on the embankment side of the piers. In order to allow for arching effects, Chettoe and Adams suggested replacing the true width, d, of the pier by an effective width, E d, as shown in Figure 2. No explicit guidance was offered on the precise choice of the value of E, except that it should lie between 1 and 2.

To evaluate the adequacy of the Chettoe and Adams approach, and to provide guidance on the choice of the factor, E, (that is, on the effective width to be taken for the piers) a

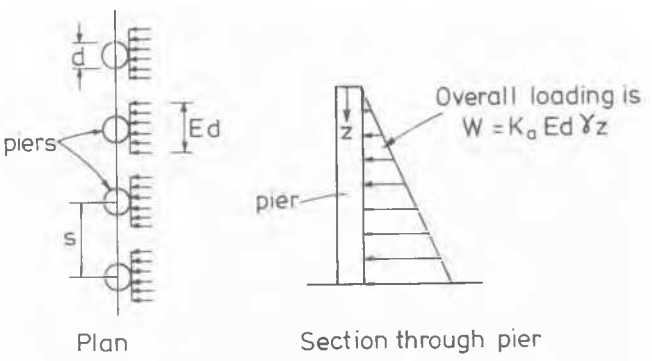

Fig. 2 Chettoe and Adams Design Approach

series of centrifuge model tests has been performed. The object of the tests was to consider limiting conditions, where support offered by the sloping side of the embankment was partially removed. The test results have led to a proposed new design approach, based on this particular limit state, which takes due account of the spacing and flexibility of the piers, and where some allowance may be made for the stress state induced during construction of the embankment.

CENTRIFUGE TESTS

Figure 3 shows a drawing of the package used for the centrifuge tests. The aluminium base of the embankment, which was roughened by gluing sandpaper to it, was designed to allow different geometries of piers (varying in number, spacing and cross-sectional shape) to be incorporated. The piers were situated at the crest of the slope in all the tests. The desired limit state was achieved by means of a horizontal sliding plate beneath the sloping side of the embankment. At the appropriate stage during the test, the plate could be moved at a rate of about 12 mm/min, by

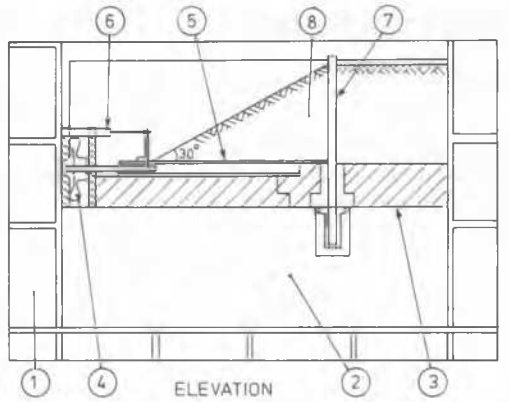

Fig. 3 Centrifuge Testing Package

up to 12 mm away from the line of piers. Table I gives the dimensions of the apparatus.

The sand used in the tests was dry 18/36 Leighton Buzzard sand, with average voids ratios of 0.52 for the 'dense' tests, and 0.75 for the 'loose' tests. For the dense tests, the estimated peak angle of friction for the sand was 48.5°, while the critical state angle was 33°. Sheets of glass were placed either side of the embankment in order to minimise friction. James (1965) quotes friction angles of about 4.5° between sand and glass.

Both circular and rectangular piers were strain gauged internally with 8 pairs of strain gauges, arranged to indicate bending strain in the piers. Movement of the sliding plate was monitored by a standard displacement transducer (LVDT in Fig. 3). Movements and strains within the embankment were estimated from photographs, taken in-flight, of the side of the embankment in which was embedded a grid of silvered nylon markers.

Ah-Teck (1983) has described the testing procedure in detail. Essentually a test consisted

TABLE I

Dimension of Centrifuge Package

		Model	Prototype
Embankment:	Slope	- 30°	30°
	Heights	- 100 mm	4.0 m
		150 mm	6.0 m
		225 mm	9.0 m
	Width	- 190 mm	7.6 m
Piers: (Circular)			
Outer diameter		- 15 mm	0.6 m
Wall thickness		- 0.91 mm	37 mm
Bending Rig'y (EI)		- 75 Nm^2	192 MN^2
(Rectangular)			
Width (across)		- 13 mm	0.78 m
Breadth (along)		- 20 mm	1.28 m
Bending Rig'y (EI)		- 20 Nm^2	259 MNm^2

of accelerating the preformed embankment to the appropriate acceleration level (40 g for the circular piers, and 60 g for the rectangular piers), noting the bending moment distribution in the piers at that stage, and then forcing the limit state event by sliding the horizontal plate away from the line of piers. During this last stage, photographs were taken at regular intervals, and the bending strains in the piers were recorded continuously on an analogue magnetic tape recorder.

It was found that the bending moments induced in the piers under normal 'working conditions' (with no movement of the sliding plate) were negligible. However, only small movements (less than 3 mm) of the plate produced high bending moments that remained essentially constant with further movement of the plate. The profile of bending moments down the piers was found to be consistent with a net lateral thrust on the piers that was proportional to depth below the top of the embankment.

Table II summarises the results from twelve tests conducted for a range of values of H/d, s/d, and pier geometry for both loose and dense sand conditions. The best fit (deduced) loading on the piers, and the deflection at the pier head (Δ/H) is also tabulated, together with parameters E and k that will be discussed in the following section.

ANALYSIS

The basic approach adopted in analysing the problem is illustrated in Figure 4. Considering two planes on the embankment and down-slope sides of the line of piers, the lateral thrust on the piers arises from the difference between the normal stress acting on the two planes. On the embankment side of the piers, the horizontal

TABLE II

Summary of Test Results

Tests in dense sand:

Test No.	s/d	H/d	dW/dz (kPa)	Δ/H (%)	E	k
5	3.1	10.0	4.0	0.09	2.7	0.60
6	12.7	10.0	5.7	0.13	3.8	0.55
8	4.2	10.0	4.7	0.11	3.2	0.55
10	12.7	15.0	3.8	0.50	2.5	0.25
11	12.7	6.7	8.0	0.04	5.4	0.90
12*	6.7	10.0	5.2	0.12	3.5	0.50
13*	14.6	11.3	4.7	0.40	2.3	0.20
15	4.8	11.3	3.7	0.31	1.9	0.15

Tests in loose sand:

Test No.	s/d	H/d	dW/dz (kPa)	Δ/H (%)	E	k
7	12.7	10.0	7.7	0.18	3.0	0.70
9*	4.2	10.0	6.3	0.15	2.5	0.65
14*	14.6	11.3	7.7	0.66	2.2	0.25
16	4.8	11.3	7.0	0.60	2.0	0.35

*Rectangular piers

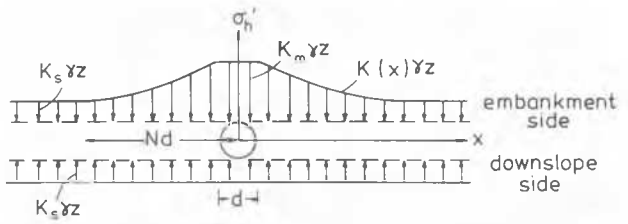

(a) Pressure distributions for single pier

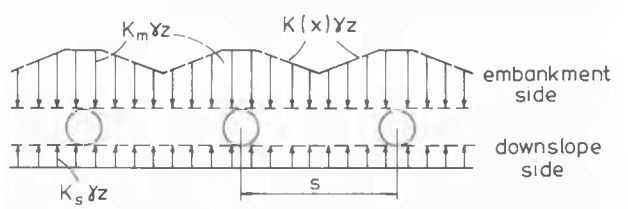

(b) Pressure distributions for closely spaced piers

Fig. 4 Postulated Pressure Distributions

Optimising this equation for $\beta = 30^o$ and $\phi' = 48.5^o$ gives $\theta = 22^o$ and $P\cos\phi' = 0.0828\ \gamma H^2/2$. Thus the value of K_s is 0.0828. The value of θ agrees well with the measured angle of 21^o.

A similar procedure can be adopted for loose sand, taking $\phi' = 33^o$, which leads to a value of $K_s = 0.166$.

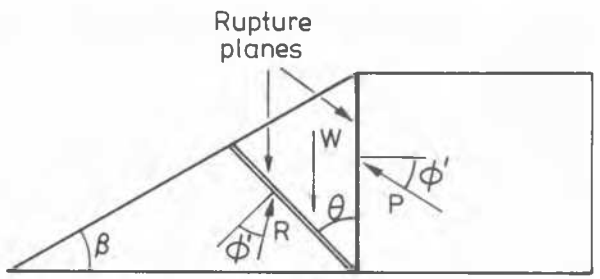

Fig. 5 Postulated wedge failure

stresses may be considered to vary between a maximum value of $\sigma_h' = K_m\gamma z$ just behind each pier, down to a minimum value of $K_s\gamma z$ some distance away from the pier (γz being the vertical stress at depth z). On the downslope side of the piers it has been assumed that a uniform value of normal stress of $\sigma_h' = K_s\gamma z$ acts. Where piers are spaced closer than some value N diameters, the pressure distribution will be more as shown in Fig. 4(b).

The maximum value of normal stress, $K_m\gamma z$, will depend on the construction method (that is, on the initial value of K_o induced during construction) as well as on the flexibility of the piers, which determines the magnitude of the movements prior to the limit state event. In most cases, the deflection at the top of the piers is quite small, with values of Δ/H ranging between 0.04 and 0.66%. Mak (1984) has found that active conditions do not develop behind retaining walls until movements of the order of 0.5% of the wall height. For smaller movements, the value of K_m will lie between the in situ value, K_o, and the Rankine active value, K_a. It is convenient to introduce a variable k, defined as

$$k = (K_m - K_a)/(K_o - K_a) \qquad (1)$$

which will denote to what extent the stress state behind the piers has reduced from the in situ condition to an active condition.

The minimum value of normal stress, $K_s\gamma z$, will be determined by the failure conditions of a wedge of soil on the immediate down-slope side of the piers. The equilibrium of the wedge of soil may be considered as shown in Figure 5, from which the horizontal component of the active force P may be shown to be

$$P\cos\phi' = \frac{\gamma H^2}{2} \frac{\cos\phi' \cos(\theta + \phi')}{(\cot\theta + \tan\beta)\sin(\theta + 2\phi')} \qquad (2)$$

The final part of the analysis lies in estimating how rapidly the normal stresses on the embankment side of the pier reduce from $K_m\gamma z$ to to $K_s\gamma z$. From the test results, it was found that piers spaced wider apart than about 8 diameters showed no interaction. Thus the value of N in Figure 4(a) may be taken as 4. In addition, Ah-Teck (1983) showed that a variation in normal stress that was proportional to the 2/3 power of distance from the pier gave best agreement with the test results. Thus the value of normal stress as a distance x from the pier centreline may be expressed as $\sigma_h' = K(x)\gamma z$, where

$$K(x) = K_m \qquad 0 \leq x \leq d/2$$

$$K(x) = K_m - (K_m - K_s)\left[(x/d - 0.5)/3.5\right]^{2/3} \qquad d/2 \leq x \leq 4d$$

$$K(x) = K_s \qquad x \geq 4d$$

For widely spaced piers (greater than 8d), the net force, W, on each pier may be evaluated by integration as

$$W = 3.8\ (K_m - K_s)d\gamma z \qquad (3)$$

while for more closely spaced piers,

$$W = (K_m - K_s)d\gamma z\ \left[s/d - 0.164(s/d - 1)^{5/3}\right]$$

In order to compare the above approach with the original Chettoe and Adams approach, it is helpful to recast the above results in terms of active pressures acting on an effective width E d. This may be achieved by dividing the above expressions by $K_a d\gamma z$ to give

$$E = \left[s/d - 0.164(s/d - 1)^{5/3}\right](K_m - K_s)/K_a \qquad \text{for } s/d \leq 8$$

$$E = 3.8\ (K_m - K_s)/Ka \qquad \text{for } s/d \geq 8$$

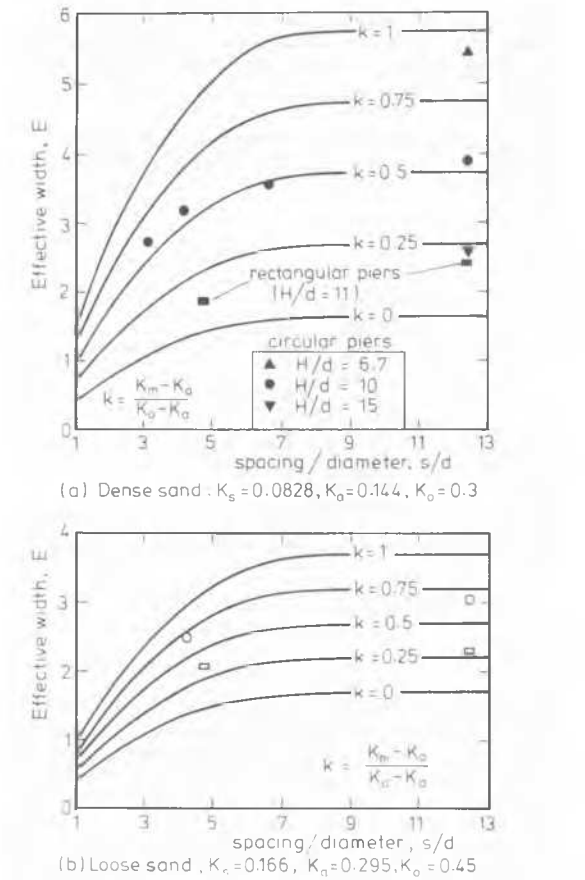

Fig. 6 Design Chart for Effective Width

These expressions may be plotted in the form of design charts, for given values of K_o, K_a and K_s as shown in Figure 6. The actual test results are plotted on the curves and enable the deduced values of k to be correlated with the movement at the head of the pier. This correlation is shown in Figure 7. It may be seen that the test data fall in two bands, one for dense sand and one for loose sand. It would appear that, for movements less than Δ/H = 0.03% (dense) or 0.06% (loose) earth pressures behind the piers remain at the in situ value, while for movements greater than Δ/H = 0.6% (dense) or 2.0% (loose), the pressures may be taken as the active value.

The possibility of high pressures remaining locked behind the piers points to a potential disadvantage in the use of heavy construction plant operating behind the piers during construction. The expressions for the net lateral thrust on the piers show W proportional to the difference between K_m and K_s. This difference will be largest for well compacted fill behind stiff piers, and steep angles of the sloping part of the embankment (which will give low values of K_s)

CONCLUSIONS

The results presented in this paper are relatively restricted in scope, and need to be verified by more data, preferably from field

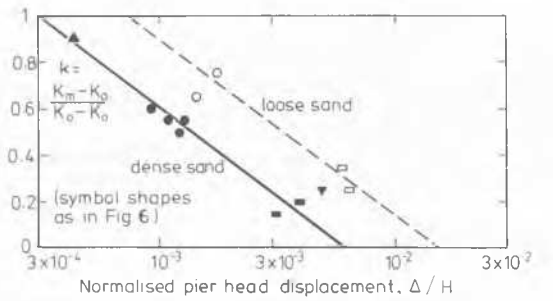

Fig. 7 Variation of k with Pier Movement

trials, before the design method can be verified in detail. However, it is considered that the overall approach of considering the differential pressures acting on the two sides of the line of piers, is a more rational approach to the design of spill-through abutments than that proposed by Chettoe and Adams (1938).

REFERENCES

Ah-Teck, C Y (1983). The Behaviour of Spill-Through Abutments. M.Phil. Thesis, University of Cambridge

Chettoe, C S and Adams, H C (1938). Reinforced Concrete Bridge Design (2nd Edition), Chapman and Hall, London

James, R G (1965). Stress and strain fields in sand. PhD Thesis, University of Cambridge

Mak, K W (1984). Modelling the effects of strip loads behind rigid retaining walls, PhD Thesis, University of Cambridge

ACKNOWLEDGEMENT

The work described in this Paper was carried out at Cambridge University under contract to the Transport and Road Research Laboratory (TRRL) and is published by permission of the Director of TRRL. Any views expressed in this Paper are not necessarily those of the Department of the Environment or the Department of Transport.